Vinyl-polyethylene waxes with narrow dispersity using a thermally robust bis(imino)trihydroquinolyl-chromium catalyst

Chuanbing Huang,[a,b] Youfu Zhang,[a,c] Gregory A. Solan,[*,a,d] Yanping Ma,[a] Xinquan Hu,[*,c] Yang Sun[a] and Wen-Hua Sun[*a,b]

Abstract: Five structurally related chromium(III) complexes, [2-(ArNCMe)-8-(NAr)C_9H_8N]$CrCl_3$ (Ar = 2,6-Me_2Ph **Cr1**, 2,6-Et_2Ph **Cr2**, 2,6-*i*-Pr_2Ph **Cr3**, 2,4,6-Me_3Ph **Cr4**, 2,6-Et_2-4-MePh **Cr5**), each bearing an unsymmetrical bis(imino)trihydroquinoline ligand, have been synthesized in good yield and fully characterized. The molecular structure of **Cr2** reveals a distorted octahedral geometry at the metal center with the sterically bulky N,N,N-ligand adopting a *mer*-configuration. On activation with MAO or MMAO, **Cr1** – **Cr5**, were highly active catalysts for ethylene polymerization operating most effectively at 80 °C (up to 15.96 × 10^6 g (PE)·mol^{-1} (Cr)·h^{-1}); even at 100 °C the activity still maintained a good level (2.92 × 10^6 g (PE)·mol^{-1} (Cr)·h^{-1}). Highly linear polyethylene waxes of low molecular weight and narrow distribution (1.1 – 1.8), incorporating predominantly vinyl/methyl and some methyl/methyl end-groups, are a feature of the materials obtained. The influence of steric/electronic changes to the pre-catalyst and polymerization reaction parameters on both the catalytic activities as well as the properties of the polymeric product has been the subject of a detailed investigation.

Introduction

Transition metal catalysts have a longstanding record for their role in the production of polyolefins.[1] Among the many types of transition metals employed, systems based on chromium have distinguished themselves for their extensive applications in ethylene oligomerization and polymerization,[1d,1e,2] with both heterogeneous[1e,1f] and homogeneous variants common place. Given the versatility of this metal in polymerization applications, considerable research effort has been directed towards ligand development with a view to improving the stability and catalytic activity of the active species.[3] In particular, tridentate ligands based on a wide variety of donor group combinations such as N,N,N,[4] N,N,O,[5] N,S,N,[6] P,P,P,[7] P,N,P,[8] S,N,S[9] and C,N,C[10] have emerged in the literature. With regard to the N,N,N-based bis(imino)pyridine, their chromium(III) pre-catalysts generate polyethylenes that characteristically display high linearity or contain some short chain branching (**A**, Scheme 1).[11] Further developments of the bis(imino)pyridine frame through the fusion of one or two cycloalkyl groups to the central pyridine donor have seen, for late transition metals (*e.g.,* iron and cobalt), notable effects on not only the catalytic activity but also on the properties of the polymer itself.[12] Recently, *α,α′*-bis(arylimino)-2,3:5,6-bis(pentamethylene)pyridyl-chromium(III) chloride complexes possessing a central pyridine fused by two seven-membered rings have been reported as highly active pre-catalysts affording either high density polyethylene (HDPE) or vinyl-polyethylene waxes depending on the co-catalyst used (**B**, Scheme 1).[13] In addition, chromium complexes incorporating the more strained 2-(1-aryliminoethyl)-7-arylimino-6,6-dimethyl cyclopenta*[b]*pyridine exhibit good activities towards ethylene polymerization affording strictly linear polyethylenes (**C**, Scheme 1).[14]

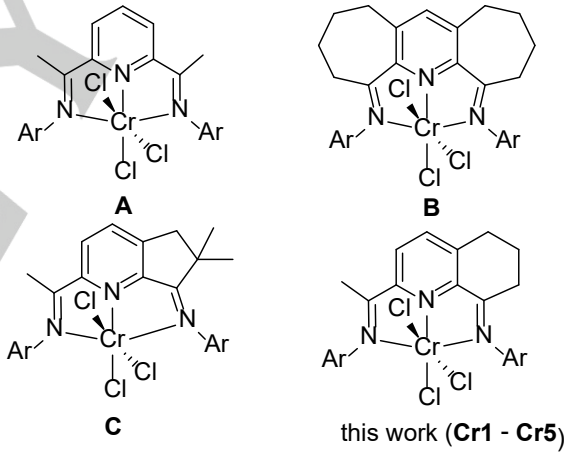

Scheme 1. Development of the parent bis(imino)pyridyl-Cr(III) pre-catalyst, **A**, through incorporation of fused cycloalkyl units

In this article, we are concerned with exploring the effect of integrating a cyclohexyl moiety into the parent bis(imino)pyridine ligand frame on catalytic performance of the resulting chromium pre-catalyst. In particular, we disclose the synthetic and characterization details for a series of novel 2-(1-(arylimino)ethyl)-8-arylimino-5,6,7-trihydroquinolinyl-chromium(III) chlorides (**Cr1** – **Cr5**, Scheme 1) that differ in both the steric and electronic properties of the N-aryl groups. A detailed catalytic evaluation of the complexes is then performed to identify the most suitable co-catalyst, operating temperature and co-catalyst/pre-catalyst molar ratio to deliver the most effective conditions for the polymerization. Influences on the resulting polymeric material will be correlated with steric/electronic features of the ligand frame as well as the reaction parameters employed; comparisons of these findings

[a] Mr. C. Huang, Mr. Y. Zhang, Prof. G. A. Solan, Dr. Y. Ma, Miss Y. Sun, Prof. W.-H. Sun*
Key Laboratory of Engineering Plastics and Beijing National Laboratory for Molecular Sciences
Institute of Chemistry, Chinese Academy of Sciences
Beijing 100190, China.
E-mail: whsun@iccas.ac.cn
[b] Mr. C. Huang, Prof. W.-H. Sun*
CAS Research/Education Center for Excellence in Molecular Sciences
University of Chinese Academy of Sciences
Beijing 100049, China
[c] Mr. Y. Zhang, Prof. X. Hu
College of Chemical Engineering
Zhejiang University of Technology
Hangzhou 310014, China
Email: xinquan@zjut.edu.cn
[d] Prof. G. A. Solan
Department of Chemistry
University of Leicester
University Road, Leicester LE1 7RH, UK
E-mail: gas8@leicester.ac.uk.

Supporting information for this article is given via a link at the end of the document.

with those previously observed using **A** – **C** (Scheme 1) and related pre-catalysts will be discussed.

Results and Discussion

Synthesis and characterization

The chromium(III) complexes, [2-(ArN=CMe)-8-(NAr)C_9H_8N] $CrCl_3$ (Ar = 2,6-Me_2Ph **Cr1**, 2,6-Et_2Ph **Cr2**, 2,6-*i*-Pr_2Ph **Cr3**, 2,4,6-Me_3Ph **Cr4**, 2,6-Et_2-4-MePh **Cr5**), can be obtained in high yield (80 - 92%) by the reaction of $CrCl_3(THF)_3$ with the corresponding tautomeric mixture of 2-(ArN=CMe)-8-(NAr)C_9H_8N (Ar = 2,6-Me_2Ph **L1**, 2,6-Et_2Ph **L2**, 2,6-*i*-Pr_2Ph **L3**, 2,4,6-Me_3Ph **L4**, 2,6-Et_2-4-MePh **L5**) and 2-(ArN=CMe)-8-(NHAr)C_9H_7N (Ar = 2,6-Me_2Ph **L1'**, 2,6-Et_2Ph **L2'**, 2,6-*i*-Pr_2Ph **L3'**, 2,4,6-Me_3Ph **L4'**, 2,6-Et_2-4-MePh **L5'**) in acetone at reflux (Scheme 2).[14] Compounds **L1**/**L1'** – **L5**/**L5'** have been previously reported and shown to exist in solution in both the imine and enamine forms.[12b] All new complexes have been characterized by IR spectroscopy and elemental analysis. In addition **Cr2**, as a representative example, has been the subject of a single crystal X-ray diffraction study.

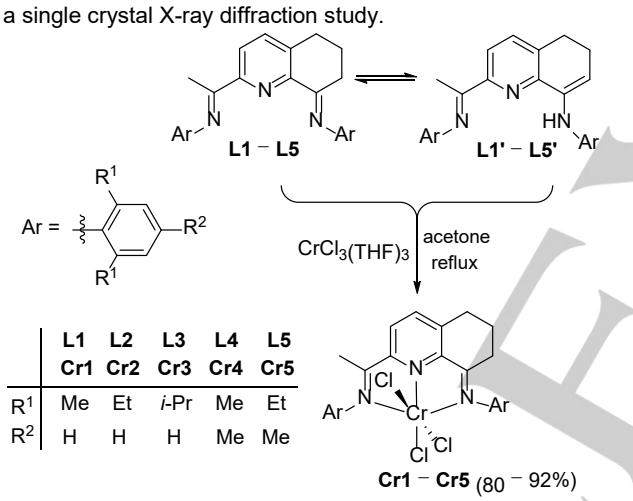

	L1 Cr1	L2 Cr2	L3 Cr3	L4 Cr4	L5 Cr5
R^1	Me	Et	*i*-Pr	Me	Et
R^2	H	H	H	Me	Me

Scheme 2. Synthetic route to **Cr1** – **Cr5**

Crystals of **Cr2** suitable for the X-ray determination were grown by the slow diffusion of heptane into a saturated dichloromethane solution at room temperature. The molecular structure is shown in Figure 1; selected bond lengths and angles are collected in Table 1. The structure consists of a chromium center surrounded by three nitrogen donors belonging to the 2,8-diarylimino-5,6,7-trihydroquinoline ligand and three chloride ligands to complete a geometry best described as distorted octahedral. The N,N,N-ligand adopts a *mer*-configuration with the plane containing the three nitrogen atoms almost perpendicular to the plane incorporating the three chlorides. Close inspection of the octahedral arrangement reveals Cl2, Cl3, N1 and N3 fill the equatorial sites while N2 and Cl1 the axial ones (N2–Cr1–Cl1 174.37(11)°). Similar structural features have been observed elsewhere for related chromium complexes.[4d,4e,13-15] As a general feature, the planes adopted by the two N-2,6-diethylphenyl groups are inclined towards orthogonal with respect to the N,N,N coordination plane as is evidenced by the dihedral angles: 82.12° (for the plane based on C12, C13, C17) and 75.83° (for the plane based on C22, C23, C27). Of the three Cr-N distances, the one involving the central pyridine is the shortest [Cr1-N2 1.985(4) Å], in accord with the stronger binding of this unit compared to the exterior N_{imine} donors. Some deviation is also observed between the two Cr–N_{imine} bond lengths [Cr1-N1 2.137(4) vs. Cr1-N3 2.173(3) Å] which can be attributed to the unsymmetrical nature of the ligand framework;[14] similar observations have been noted with their cobalt and iron counterparts.[12] In addition, the Cr–$N_{pyridyl}$ bond length (1.985(4) Å) is shorter than the corresponding distance in these iron(II) (2.069 Å)[12b] and cobalt(II) (2.051 Å)[12c] complexes, highlighting the more effective binding with the higher oxidation state Cr(III) center.

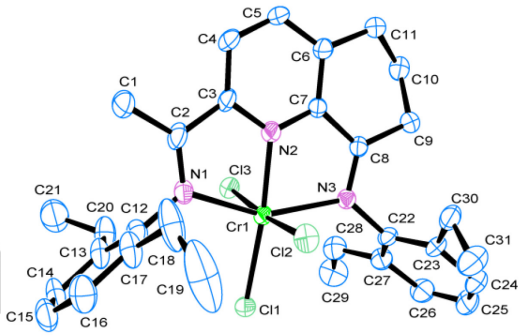

Figure 1. ORTEP drawing of complex **Cr2**. Thermal ellipsoids are shown at the 30% probability level and H atoms are omitted for clarity.

Table 1. Selected bond lengths (Å) and angles (°) for **Cr2**

Bond lengths (Å)			
Cr(1)−N(1)	2.137(4)	Cr(1)−Cl(2)	2.3021(15)
Cr(1)−N(2)	1.985(4)	Cr(1)−Cl(3)	2.3324(14)
Cr(1)−N(3)	2.173(3)	N(1)−C(2)	1.288(6)
Cr(1)−Cl(1)	2.2813(13)	N(3)−C(8)	1.297(5)
Bond angles (°)			
N(1)−Cr(1)−N(3)	153.33(14)	N(2)−Cr(1)−Cl(2)	92.12(12)
N(1)−Cr(1)−N(2)	76.74(15)	N(2)−Cr(1)−Cl(3)	83.22(12)
N(2)−Cr(1)−N(3)	76.97(14)	N(3)−Cr(1)−Cl(1)	106.41(10)
N(1)−Cr(1)−Cl(1)	100.15(11)	N(3)−Cr(1)−Cl(2)	86.81(10)
N(1)−Cr(1)−Cl(2)	89.74(12)	N(3)−Cr(1)−Cl(3)	89.46(10)
N(1)−Cr(1)−Cl(3)	91.85(12)	C(2)−N(1)−Cr(1)	114.5(3)
N(2)−Cr(1)−Cl(1)	174.37(11)	C(8)−N(3)−Cr(1)	113.0(3)

The FT-IR spectra for **Cr1** – **Cr5** in each case show $\nu_{C=N}$ stretching frequencies falling in the range 1612 – 1627 cm^{-1}. In

comparison with **L1** – **L5**, these imine bands are shifted to lower wavenumber (*ca.* 20 cm^{-1}), supportive of the coordination between the imine-nitrogen atoms and the chromium center. No evidence for an N-H stretch could be detected in their IR spectra in agreement with the tridentate ligand adopting solely the bis-imine form on coordination to the metal center. Consistent microanalytical data lend further support for the elemental composition given for **Cr1** – **Cr5**.

Ethylene Polymerization Studies

Co-catalyst screen

In the first instance **Cr2** was evaluated as the test pre-catalyst so as to identify to most suitable co-catalyst. Four different alkylaluminum reagents, namely methylaluminoxane (MAO), modified methylaluminoxane (MMAO), ethylaluminum sesquichloride ($Et_3Al_2Cl_3$, EASC) and diethylaluminum chloride (Et_2AlCl) were assessed with each run being performed at 10 atmospheres of ethylene pressure, at 30 °C and over 30 minutes; the results are compiled in Table 2. All polymeric materials were characterized by gel permeation chromatography (GPC) and differential scanning calorimetry (DSC); gas chromatography was also performed to detect any oligomers. Inspection of the data (entries 1 – 4, Table 2) reveals that the use of MAO and MMAO showed the best catalytic activities along with the lowest molecular weights and narrowest distributions for the resultant polymers. On the basis of these results, co-catalysts MAO and MMAO were selected for further more detailed investigations.

Table 2. Catalytic evaluation of **Cr2** with a range of aluminum-alkyl co-catalysts [a]

Entry	Co-catalyst	Al/Cr	Mass, g	Activity [b]	T_m [c], °C	M_w [d]	M_w/M_n [d]
1	MAO	2000	0.83	0.42	125.7	0.77	1.22
2	MMAO	2000	2.96	1.48	86.5	0.65	1.17
3	EASC	500	0.12	0.06	137.0	269.65	67.27
4	Et_2AlCl	500	0.08	0.04	137.3	409.05	87.84

[a] General conditions: 4 μmol of **Cr2**, 30 °C, 30 min., 10 atm. of ethylene, 100 mL of toluene; [b] 10^6 g (PE)·mol^{-1} (Cr)·h^{-1}; [c] Determined by DSC; [d] M_w: 10^3 g mol^{-1}, determined by GPC.

Catalytic evaluation using Cr1 – Cr5/MAO

To explore the influence of the reaction parameters such as Al/Cr molar ratio, reaction temperature and reaction time on the polymerization, **Cr2** was again selected for a more in-depth investigation in this case using MAO as the co-catalyst; the results are collected in Table 3.

Firstly, the effect of varying the Al/Cr molar ratio was investigated with the temperature of the run maintained at 30 °C. On increasing the ratio from 1000 to 2000 over a 30 minute time period (entries 1 – 5, Table 3), the optimal activity for **Cr2** was observed at 1500 (entry 3, Table 3). Further increasing the Al/Cr molar ratio, resulted in the molecular weight of the polymers decreasing; this latter observation is likely due to large concentrations of co-catalyst enhancing chain transfer from the active chromium species to the aluminum co-catalyst leading to shorter chain polymers.[13,16] This molecular weight trend is illustrated by the GPC curves at five different Al/Cr molar ratios (Figure 2). It is noteworthy that narrow molecular weight distributions were exhibited by all the polymers obtained (1.22 – 1.27), indicative of single-site behavior for the active species.[17]

Secondly, with the Al/Cr molar ratio fixed at 1500, the reaction temperature was increased from 20 to 100 °C (entries 3 and 6 – 12, Table 3). The highest activity for **Cr2** of 9.46 × 10^6 g (PE)·mol^{-1} (Cr)·h^{-1} was achieved at 80 °C, raising the temperature further led to a steady decrease in activity but nonetheless even at 100 °C a remarkably good level of 4.64 × 10^6 g (PE)·mol^{-1} (Cr)·h^{-1} was observed, reflecting the thermal stability of the active species. With regard to the properties of the polyethylenes, lower molecular weights and narrower distributions were evident at lower reaction temperature (20 – 30 °C), features which can likely be attributed to the low rates of chain propagation and chain transfer at these reaction temperatures. Raising the reaction temperature from 50 to 100 °C, resulted in the molecular weights of the polyethylenes slightly increasing while their distributions showed some broadening; similar melting temperatures (116.0 – 119.9 °C) were apparent over the range.

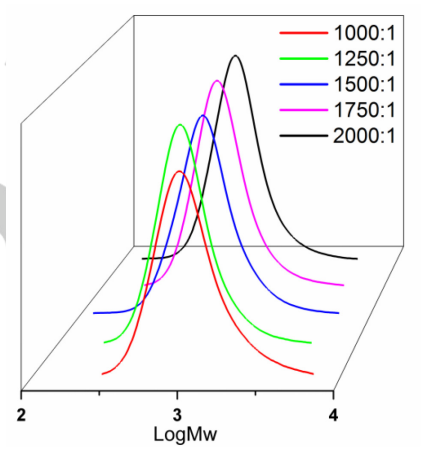

Figure 2. GPC curves for the polyethylenes obtained using **Cr2**/MAO at various Al/Cr ratios (entries 1 – 5, Table 3)

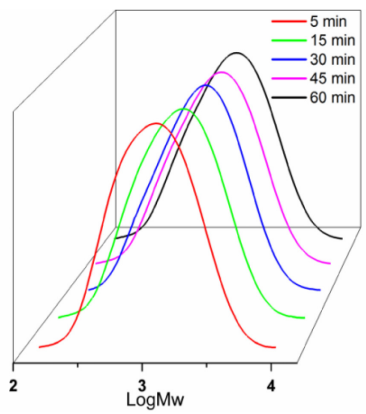

Figure 3. GPC curves for the polyethylenes obtained using Cr2/MAO over different reaction times (entries 10 and 13 – 16, Table 3).

Table 3. Screening **Cr1** – **Cr5**/MAO for ethylene polymerization [a]

Entry	Pre-catalyst	T, °C	Al/Cr	t, min	Mass, g	Activity [b]	T_m [c], °C	M_w [d]	M_w/M_n [d]
1	**Cr2**	30	1000	30	0.55	0.28	128.9	0.79	1.22
2	**Cr2**	30	1250	30	0.65	0.33	127.1	0.81	1.24
3	**Cr2**	30	1500	30	1.16	0.58	123.4	0.84	1.27
4	**Cr2**	30	1750	30	0.94	0.47	128.1	0.79	1.22
5	**Cr2**	30	2000	30	0.83	0.42	125.7	0.77	1.22
6	**Cr2**	20	1500	30	0.38	0.19	130.1	0.72	1.18
7	**Cr2**	50	1500	30	15.80	7.90	116.0	1.49	1.66
8	**Cr2**	60	1500	30	16.32	8.16	117.2	1.58	1.74
9	**Cr2**	70	1500	30	17.54	8.77	116.9	1.61	1.75
10	**Cr2**	80	1500	30	18.91	9.46	117.8	1.64	1.73
11	**Cr2**	90	1500	30	16.70	8.35	118.6	1.78	1.78
12	**Cr2**	100	1500	30	9.28	4.64	119.9	1.63	1.70
13	**Cr2**	80	1500	5	4.34	13.02	115.6	1.34	1.61
14	**Cr2**	80	1500	15	11.47	11.47	117.3	1.51	1.71
15	**Cr2**	80	1500	45	26.56	8.85	119.9	1.67	1.80
16	**Cr2**	80	1500	60	30.04	7.51	120.5	1.66	1.77
17[e]	**Cr2**	80	1500	30	7.98	3.99	117.1	1.25	1.87
18[f]	**Cr2**	80	1500	30	2.11	1.06	108.8	0.99	1.38
19	**Cr1**	80	1500	30	5.15	2.58	102.8	0.96	1.47
20	**Cr3**	80	1500	30	3.54	1.77	130.5	8.39	1.99
21	**Cr4**	80	1500	30	15.98	7.99	100.4	0.91	1.45
22	**Cr5**	80	1500	30	4.29	2.15	114.1	1.19	1.54

[a] General conditions: 4 μmol of **Cr**; 10 atm. of ethylene; 100 mL of toluene; [b] 10^6 g (PE)·mol^{-1} (Cr)·h^{-1}; [c] Determined by DSC; [d] M_W : 10^3 g mol^{-1}, determined by GPC; [e] 5 atm. of ethylene; [f] 1 atm. of ethylene.

Thirdly, to explore the lifetime of the active species derived from **Cr2**, run times of 5, 15, 30, 45 and 60 minutes (entries 3 and 13 – 16, Table 3) were conducted with the Al/Cr molar ratio kept at 1500 and the temperature at 80 °C. The best activity of 13.02 × 10^6 g (PE)·mol^{-1} (Cr)·h^{-1} was observed after 5 minutes (entry 13, Table 3), which is higher than that observed after 30 minutes (9.46 × 10^6 g (PE)·mol^{-1} (Cr)·h^{-1}, entry 10, Table 3); this would imply that the active species was quickly formed following the addition of the co-catalyst and then gradually deactivated over more extended reaction times.[13,14,18] In addition, the molecular weights of the polyethylenes were found to slightly increase over longer reaction times (Figure 3). It is worth mentioning that when the ethylene pressure was lowered from 10 atmospheres (entry 10, Table 3) to 5 or 1 atmospheres (entries 17, 18, Table 3), and the other reaction parameters kept constant, the catalytic activity dropped rapidly, but nevertheless fell within the same order of magnitude, *viz.* 10^6 g (PE)·mol^{-1} (Cr)·h^{-1}. In general, polyethylenes with higher molecular weight were produced at higher pressures of ethylene (entries 10 and 17, Table 3).

Finally, by employing the optimum conditions established for **Cr2**/MAO [Al/Cr molar ratio of 1500, reaction temperature of 80 °C and polymerization time within 30 minutes], the four other chromium(III) pre-catalysts, **Cr1**, **Cr3**, **Cr4** and **Cr5**, were screened for their catalytic performance (entries 19 – 22, Table 3). Close examination of the data showed these catalysts exhibited catalytic activities in the order: **Cr2** [2,6-di(Et)] > **Cr4** [2,4,6-tri(Me)] > **Cr1** [2,6-di(Me)] > **Cr5** [2,6-di(Et)-4-Me] > **Cr3** [2,6-di(*i*-Pr)]. It would appear that both steric and electronic effects imparted by the ligand influence catalytic performance, with the most sterically protected **Cr3** affording the lowest activity and 2,6-diethyl-containing **Cr2** the highest. Furthermore,

Cr3 generated the highest molecular weight polyethylene of the series [8.39 × 10^3 g mol^{-1}] but with the broadest distribution (Figure 4). In general, on increasing the reaction temperature and prolonging the run time, the molecular weights and polydispersities of the polymers increased leading to some slight deviation in their melting temperatures (see Table 3). In any case, the majority of melting temperatures fall within 110 and 120 °C range, which reflects the high linearity of the polymer.

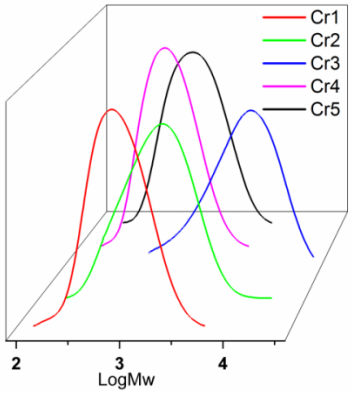

Figure 4. GPC curves for the polyethylenes obtained using **Cr1** – **Cr5**/MAO (entries 10 and 19 – 22, Table 3)

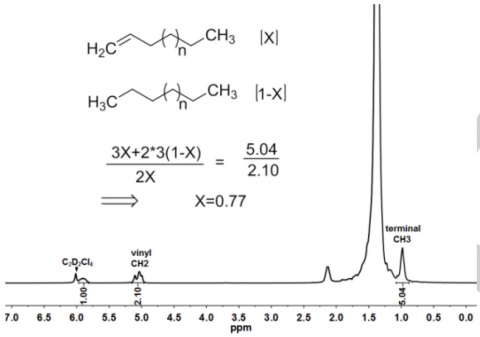

Figure 5. ^{1}H NMR spectrum of the polyethylene obtained using **Cr2**/MAO at 80 °C; recorded in 1,1,2,2-tetrachloroethane-d_2 at 100 ºC and "X" represents the molar ratio of the vinyl-PEs in the polymer mixture (entry 10, Table 3)

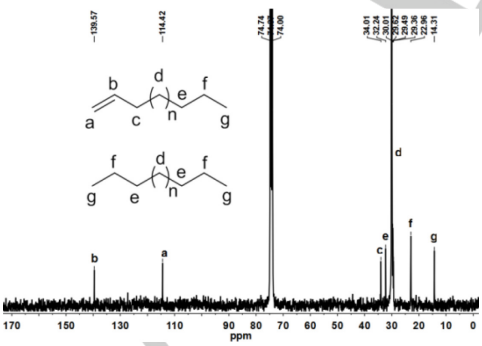

Figure 6. ^{13}C NMR spectrum of the polyethylene obtained using **Cr2**/MAO at 80 °C; recorded in 1,1,2,2-tetrachloroethane-d_2 at 100 ºC (entry 10, Table 3)

To lend further support for the microstructural features of the polymer, one representative sample obtained at 80 °C using **Cr2**/MAO (entry 10, Table 3) was characterized by high-temperature ^{1}H NMR and ^{13}C NMR spectroscopy (recorded at 100 °C in 1,1,2,2-tetrachloroethane-d_2). The observations of a prominent singlet at δ 1.30 in the ^{1}H NMR spectrum (Figure 5) along with a peak around δ 30.01 in the ^{13}C NMR spectrum (Figure 6) are consistent with strictly linear polyethylene. In addition, the more downfield peaks in the ^{1}H NMR spectrum around δ 5.90 and an apparent triplet at δ 5.00, with a relative peak area ratio of 1:2 (Figure 5), imply that the polymerization mechanism can terminate by *β*-hydride elimination or transfer with the resulting formation of chain-end vinyl groups (–CH=CH_2).[12f,12i,19] This latter finding is supported by the ^{13}C NMR spectrum which shows the corresponding peaks at δ 139.57 and δ 114.42 (Figure 6).

The number-average molecular weight, M_n = 1439 g·mol^{-1}, of the polymer can also be calculated from the ^{1}H NMR spectrum by considering the ratio of the integrals for the vinyl end-group to the methylene group.[19c] When compared to the value detected by GPC (M_n = 948 g·mol^{-1}), this value is somewhat higher. Moreover, end-group analysis of this linear polymer based on the ^{13}C NMR spectrum,[19d,19e] reveals two types namely, vinyl/methyl and methyl/methyl (see later for mechanistic discussion); the molar ratio being respectively 77/33 as determined from their characteristic hydrogen peak areas found in the ^{1}H NMR spectrum (Figure 5).

Catalytic evaluation using Cr1 – Cr5/MMAO

Cr2 was once again used as the test pre-catalyst to optimize the conditions for the polymerization this time using MMAO as the co-catalyst; the results are listed in Table 4. At first glance, the data are quite similar to that observed with **Cr2**/MAO discussed above, although the optimal Al/Cr molar ratio is now 2500 which at 80 °C gives a maximum activity of 8.73 × 10^6 g (PE)·mol^{-1} (Cr)·h^{-1} for a 30 minute run time (entry 10, Table 4). This result is slightly lower than the corresponding activity of 9.46 × 10^6 g (PE)·mol^{-1} (Cr)·h^{-1} achieved using **Cr2**/MAO (entry 10, Table 3). On the other hand, this **Cr2**/MMAO system shows higher activities at 20 or 30 °C with the polymers displaying lower melting temperatures and molecular weights as well as narrower distributions. As with the MAO-promoted system, short run times lead to increased activity with the maximum of 15.96 × 10^6 g (PE)·mol^{-1} (Cr)·h^{-1} reached after 5 minutes (entry 13, Table 4), these findings being consistent with rapid formation of the active species followed by gradual deactivation on prolonging the reaction time.[13,14,18]

All the polymeric samples obtained using **Cr2**/MMAO display a unimodal feature which is illustrated in their stacked GPC curves (Figures S1 and S2). These curves also reveal narrow distributions over a range of different polymerization conditions (*e.g.*, molar ratios of co-catalyst and reaction time). Furthermore, the values of the polydispersities (1.04 – 1.79, see Table 4) are in accord with single-site catalysts.[17] With the optimum catalytic conditions fixed at an Al/Cr molar ratio of 2500, a reaction temperature of 80 °C and a reaction time of 30 minutes, the four remaining chromium complexes, **Cr1**, **Cr3**, **Cr4** and **Cr5**, were evaluated. As with the data obtained using MAO, the activities of

Table 4 Screening **Cr1** – **Cr5**/MMAO for ethylene polymerization [a]

Entry	Pre-catalyst	T, °C	Al/Cr	t, min	Mass, g	Activity [b]	T_m [c], °C	M_w [d]	M_w/M_n [d]
1	**Cr2**	30	2000	30	2.96	1.48	86.5	0.65	1.17
2	**Cr2**	30	2250	30	4.39	2.20	90.6	0.71	1.18
3	**Cr2**	30	2500	30	4.63	2.32	88.9	0.66	1.12
4	**Cr2**	30	2750	30	3.83	1.92	86.4	0.61	1.11
5	**Cr2**	30	3000	30	3.52	1.76	85.5	0.60	1.11
6	**Cr2**	20	2500	30	3.35	1.68	87.7	0.65	1.15
7	**Cr2**	50	2500	30	14.79	7.40	112.0	1.05	1.38
8	**Cr2**	60	2500	30	15.15	7.58	110.7	1.14	1.42
9	**Cr2**	70	2500	30	16.38	8.19	113.3	1.28	1.55
10	**Cr2**	80	2500	30	17.46	8.73	114.8	1.38	1.60
11	**Cr2**	90	2500	30	9.63	4.82	112.5	1.19	1.48
12	**Cr2**	100	2500	30	5.83	2.92	115.2	0.96	1.36
13	**Cr2**	80	2500	5	5.32	15.96	107.2	0.85	1.38
14	**Cr2**	80	2500	15	8.91	8.91	110.6	0.98	1.37
15	**Cr2**	80	2500	45	21.42	7.14	115.1	1.31	1.57
16	**Cr2**	80	2500	60	23.51	5.88	115.3	1.21	1.52
17 [e]	**Cr2**	80	2500	30	8.63	4.32	115.5	1.05	1.42
18 [f]	**Cr2**	80	2500	30	3.78	1.89	114.4	0.40	1.04
19	**Cr1**	80	2500	30	6.17	3.09	117.2	0.59	1.18
20	**Cr3**	80	2500	30	2.14	1.07	123.6	1.93	1.79
21	**Cr4**	80	2500	30	4.21	2.11	88.5	0.67	1.27
22	**Cr5**	80	2500	30	3.31	1.66	109.4	0.71	1.23

[a] General conditions: 4 μmol of **Cr**; 10 atm. of ethylene; 100 mL of toluene; [b] 10^6 g (PE)·mol^{-1} (Cr)·h^{-1}; [c] Determined by DSC; [d] M_w : 10^3 g mol^{-1}, Determined by GPC; [e] 5 atm. of ethylene; [f] 1 atm. of ethylene.

all five systems generally come in the 10^6 g (PE)·mol^{-1} (Cr)·h^{-1} range (entries 10 and 19 – 22, Table 4). More specifically the activities descend in the order: **Cr2** [2,6-di(Et)] > **Cr1** [2,6-di(Me)] > **Cr4** [2,4,6-tri(Me)] > **Cr5** [2,6-di(Et)-4-Me] > **Cr3** [2,6-di(*i*-Pr)]. Notably this order mimics that seen with MAO with the exception of **Cr1** that now precedes **Cr4**, the explanation for this variation is unclear. As with the polymer obtained using **Cr3**/MAO, that produced with **Cr3**/MMAO gave polyethylene with the highest molecular weight of the series 1.93 × 10^3 g mol^{-1} and displayed the broadest distribution (Figure S3).

In general, the microstructural properties of the materials obtained with **Cr1** – **Cr5**/MMAO are assumed to resemble those obtained with MAO and indeed their melting temperatures are in agreement with linear polyethylene. To verify this assumption, a sample obtained using **Cr2**/MMAO (entry 10, Table 4) was subject of a high-temperature ^{1}H NMR and ^{13}C NMR study. Characteristically, the ^{1}H NMR spectrum shows an intense singlet peak at around δ 1.30 for the protons of the CH_2 repeat unit (Figure S4), which is corroborated by a singlet at δ 30.00 in the ^{13}C NMR spectrum (Figure S5). In addition, the vinyl end-groups (–CH=CH_2) are clearly visible with signals at δ 5.90 ppm and at δ 5.00 in the ^{1}H NMR spectrum (Figure S4),[12f,12i,19] which is supported by carbon resonances at δ 139.57 and δ 114.41 in the ^{13}C NMR spectrum (Figure S5).

The number-average molecular weight, determined from the ^{1}H NMR spectrum,[19c] is again larger (M_n = 1791 g·mol^{-1}) than that detected by GPC (M_n = 863 g·mol^{-1}), while the amount of vinyl-ended polymer ratio is reduced to 64% (*c.f.* 77% using **Cr2**/MAO). Despite using MMAO as the activator there are, as with MAO, just two types of end group combinations (*i.e.*, vinyl/methyl and methyl/methyl); no evidence for any isopropyl group could be detected in the high temperature ^{13}C NMR

spectrum. This absence of isopropyl groups has previously been noted using other MMAO-promoted chromium catalysts,[13] and may be attributed to the active species displaying a preference to transfer the higher concentration aluminum methyl.

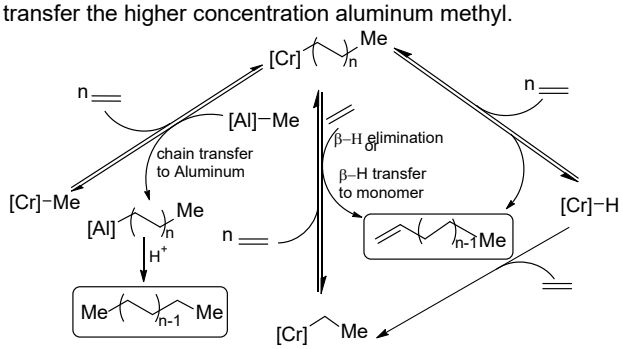

Scheme 3. Plausible chain propagation and termination pathways

With a view to accounting for the end-group variation observed for these linear polymers, we propose a mechanism for chain propagation and termination based on the one commonly accepted for bis(imino)pyridyl-chromium catalysts (Scheme 3).[11a] Firstly, propagation by a sequence of coordination/insertion steps from the active species, [Cr]-Me or [Cr]-H, generates a metallo-polymer [Cr]-$(CH_2CH_2)_n$-Me which can then undergo a *β*-hydrogen transfer to monomer (or elimination) to regenerate the active chromium-hydride and simultaneously release the free polymer containing methyl/vinyl end-groups. Alternatively, chain transfer to an [Al]-Me can occur to form an aluminum-bound polymer, [Al]-$(CH_2CH_2)_n$-Me, and at the same time re-form the active chromium-methyl species.[11a,19e] Hydrolysis of [Al]-$(CH_2CH_2)_n$-Me can then take place to give paraffinic, Me-$(CH_2CH_2)_n$-Me, containing methyl as both end-groups. From the ^{1}H NMR data for both MAO- and MMAO-promoted polymerizations, it is clear that *β*-H transfer to monomer and/or elimination is the major chain termination pathway with transfer to aluminum the minor one.

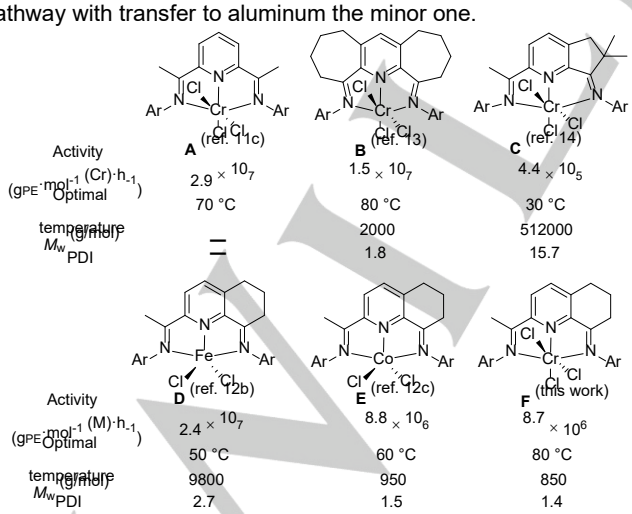

Scheme 4. Performance data for a range of related chromium (**A**, **B**, **C** and **F**) and late transition metal (**D**, **E**) pre-catalysts; MMAO as co-catalyst

Given recent interest in high temperature processes for forming low molecular weight vinyl-polyethylene waxes,[13] we view the thermally robust bis(imino)trihydroquinoline-chromium pre-catalysts developed herein as offering considerable promise. Scheme 4 highlights some performance data for the current system (**F**) when put alongside other related chromium pre-catalysts bearing 2,6-bis(imino)pyridine (**A**),[11] bis(imino)-2,3:5,6-di(pentamethylene)pyridine (**B**)[13] and bis(imino)-6,6-dimethylcyclopenta*[b]*pyridine (**C**);[14] in each case using MMAO as the co-catalyst and under otherwise comparable conditions. In addition, the findings are presented for the bis(imino)trihydroquinoline derivatives of iron (**D**) and cobalt (**E**).

Inspection of the data in Scheme 4 reveals chromium-containing **A**, **B** and **F** exhibit extremely high activities towards ethylene polymerization and reach these levels of performance only at high temperatures (70 ºC (**A**) or 80 ºC (**B** and **F**)). On the other hand, **C** achieves its optimum activity (4.4 × 10^5 g (PE)·mol^{-1} (Cr)·h^{-1}) at a much lower temperature of 30 °C. It would seem likely that the superior performance characteristics of **A**, **B** and **F** can be attributed to the effective binding of the two exterior N_{imine} donors which can afford better protection and stability to the active species at higher reaction temperatures. Indeed in **C**, there is a significant difference between the Cr–N_{imine} bond lengths with that involving the imine-nitrogen linked to the cyclopentyl unit significantly longer than its counterpart (2.299 Å *vs.* 2.150 Å).[14] In addition, **C** yields higher molecular weights (M_w = 512000 g·mol^{-1}) and broader distributions (PDI = 15.7) for the resultant polymers; it is plausible that the elongated Cr–N_{imine} bond results in some lability leading to more space around the active species and in-turn to the propagation of longer polymeric chains and more facile chain transfer. Overall **F** and **B** display the best thermal stability of the series whilst retaining high activity but yield quite different molecular weights for the polymeric materials (**F** 850 *vs.* **B** 2000 g mol^{-1}). Furthermore, when compared with iron (**D**) and cobalt (**E**), **F** exhibits better thermal stability and produces lower molecular weights as well as narrower distributions for the resultant polyethylenes; a similar trend was notably observed with the analogous Fe, Co and Cr complexes bearing 2,6-bis(imino)pyridine ligands.[11]

Conclusions

Five examples of bis(arylimino)trihydroquinolinyl-chromium(III) chlorides (**Cr1** – **Cr5**), differing in the steric/electronic properties of the N-aryl group, have been synthesized and characterized by IR spectroscopy, elemental analysis and single crystal X-ray diffraction. On activation with either MAO or MMAO, all the title complexes show optimal performance at 80 ºC for ethylene polymerization, resulting in highly linear polyethylene waxes displaying low molecular weights and narrow distributions. Furthermore, the presence of two types of end-groups (*i.e.*, vinyl/methyl and methyl/methyl) indicates that two termination mechanisms are operative with *β*-hydrogen transfer to monomer (or elimination) the dominant one. In comparison with related chromium systems, the current family of catalysts offer

exceptional thermal stability whilst maintaining high catalytic activity and afford olefinic waxes that have some industrial demand as new co-monomers.

Experimental Section

General procedures

All operations, including with air and/or moisture sensitive compounds, were performed under an atmosphere of nitrogen using standard Schlenk techniques. Prior to use, toluene was refluxed over sodium-benzophenone and distilled under nitrogen. Methylaluminoxane (MAO, 1.46 M solution in toluene) and modified methylaluminoxane (MMAO, 2.0 M solution in *n*-heptane) were purchased from Akzo Nobel Corp, while ethylaluminium sesquichloride (EASC, 0.87 M in *n*-hexane) and diethylaluminium chloride (Et_2AlCl, 1.17 M in toluene) from Acros Chemical. High-purity ethylene was supplied by Beijing Yanshan Petrochemical Co. and used as received. Other reagents were obtained from Aldrich, Acros or local suppliers. NMR spectra were recorded on a Bruker DMX 400 MHz instrument at ambient temperature using TMS as an internal standard. IR spectra were recorded on a Perkin-Elmer System 2000 FT-IR spectrometer. Elemental analysis was carried out using a Flash EA 1112 microanalyser. Molecular weights (M_W) and molecular weight distributions (M_W/M_n) of the polyethylenes were determined using an Agilent PL-GPC220 GPC/SEC high temperature instrument; three 300 × 7.5 mm PL gel 10 μm MIXED-B LS columns were employed that were connected in series. The measurements were performed at 150 °C with a flow rate of 1.0 mL min^{-1} using 1,2,4-trichlorobenzene (TCB) as the eluent. Data collection and handling were carried out using Cirrus GPC Software and Multi Detector Software. Data were collected at 1 point per second. The calibrations for constructing conventional calibration were undertaken using a Polystyrene Calibration Kit S-M-10 supplied by PL Company. The true average molecular weights of the PE were determined by inputting the *M–H* constants of PE; *K* of 0.727 and *α* of 40.6 were provided by PL Company. Samples were dissolved at a concentration of 0.5 – 2.5 mg mL^{-1}, depending on the molecular weights. The melting points of the polyethylenes were measured from the second scanning run on a PerkinElmer TA-Q2000 differential scanning calorimetry (DSC) analyzer under a nitrogen atmosphere. In the procedure, a sample of about 5.0 mg was heated to 160 °C at a rate of 20 °C/min., kept for 2 min. at 160 °C to remove the thermal history and then cooled at a rate of 20 °C/min to −40 °C. ^{13}C NMR spectra of the polyethylenes were recorded on a Bruker DMX 300 MHz instrument at 100 °C in deuterated 1,1,2,2-tetrachloroethane with TMS as an internal standard. A VARIAN CP-3800 gas chromatograph equipped with a flame ionization detector and a 30 m column (0.2 mm inert diameter, 0.25 μm film thickness) was employed to detect any oligomers in the reaction mixture. Compounds **L1**/**L1'** – **L5**/**L5'** and $CrCl_3(THF)_3$ were made using the literature methods.[12b,20]

Synthesis of [2-{(2,6-Me_2Ph)N=CMe}-8-{N(2,6-Me_2Ph)}C_9H_8N]$CrCl_3$ (Cr1). $CrCl_3(THF)_3$ (0.169 g, 0.45 mmol) was added to a tautomeric mixture of **L1** and **L1′** (0.198 g, 0.5 mmol) in acetone (10 mL). The solution was stirred and heated to reflux for 5 h and then allowed to cool to room temperature. Excess diethyl ether was poured into the reaction mixture and the resulting precipitate collected by filtration, washed with diethyl ether (3 × 5 mL) and dried under reduced to give the product as a brown powder (0.213 g, 85%). FT-IR (cm^{-1}): 2970 (m), 2920 (m), 2869 (m), 1695 (w), 1620 (m, $\nu_{C=N}$), 1578 (s), 1528 (s), 1472 (vs), 1379 (m), 1271 (m), 1250 (w), 1185 (w), 1095 (w), 1033 (w), 893 (w), 833 (w), 771 (vs), 661 (m). Anal. Calcd for $C_{27}H_{29}N_3Cl_3Cr$ (554): C, 58.55; H, 5.28; N, 7.59. Found: C, 58.47; H, 5.61; N, 7.55.

Synthesis of [2-{(2,6-Et_2Ph)N=CMe}-8-{N(2,6-Et_2Ph)}C_9H_8N]$CrCl_3$ (Cr2). Based on the procedure described for **Cr1**, using **L2**/**L2′** (0.226 g, 0.5 mmol) and $CrCl_3(THF)_3$ (0.169 g, 0.45 mmol), **Cr2** was isolated as a green powder (0.218 g, 80%). FT-IR (cm^{-1}): 2965 (m), 2928 (m), 2863 (m), 1693 (w), 1615 (m, $\nu_{C=N}$), 1579 (s), 1525 (s), 1471 (vs), 1370 (m), 1300 (m), 1265 (m), 1183 (m), 1094 (m), 1033 (w), 892 (w), 844 (w), 771 (vs), 660 (s). Anal. Calcd for $C_{31}H_{37}N_3Cl_3Cr$ (610): C, 61.04; H, 6.11; N, 6.89. Found: C, 60.94; H, 6.17; N, 6.87.

Synthesis of [2-{(2,6-*i*-Pr_2Ph)N=CMe}-8-{N(2,6-*i*-Pr_2Ph)}C_9H_8N]$CrCl_3$ (Cr3). Based on the procedure described for **Cr1**, using **L3**/**L3′** (0.254 g, 0.5 mmol) and $CrCl_3(THF)_3$ (0.169 g, 0.45 mmol), **Cr3** was isolated as a brown powder (0.261 g, 87%). FT-IR (cm^{-1}): 2961 (vs), 2928 (s), 2867 (s), 1695 (w), 1627 (m, $\nu_{C=N}$), 1569 (s), 1509 (s), 1463 (vs), 1437 (s), 1364 (s), 1323 (m), 1266 (m), 1246 (m), 1180 (m), 1101 (w), 1050 (w), 934 (m), 832 (m), 802 (s), 780 (s), 745 (m). Anal. Calcd for $C_{35}H_{45}N_3Cl_3Cr$ (666): C, 63.11; H, 6.81; N, 6.31. Found: C, 63.06; H, 6.87; N, 6.26.

Synthesis of [2-{(2,4,6-Me_3Ph)N=CMe}-8-{N(2,4,6-Me_3Ph)}C_9H_8N]$CrCl_3$ (Cr4). Based on the procedure described for **Cr1**, using **L4**/**L4′** (0.211 g, 0.5 mmol) and $CrCl_3(THF)_3$ (0.169 g, 0.45 mmol), **Cr4** was isolated as a brown powder (0.237 g, 91%). FT-IR (cm^{-1}): 2964 (s), 2918 (s), 2864 (s), 1693 (m), 1614 (m, $\nu_{C=N}$), 1575 (s), 1516 (s), 1481 (vs), 1372 (s), 1335 (m), 1270 (m), 1206 (m), 1180 (m), 1147 (w), 1116 (w), 1031 (w), 931 (w), 853 (vs), 813 (w), 764 (w). Anal. Calcd for $C_{29}H_{33}N_3Cl_3Cr$ (582): C, 59.85; H, 5.72; N, 7.22. Found: C, 59.77; H, 5.83; N, 7.14.

Synthesis of [2-{(2,6-Et_2-4-MePh)N=CMe}-8-{N(2,6-Et_2-4-MePh)}C_9H_8N]$CrCl_3$ (Cr5). Based on the procedure described for **Cr1**, using **L5**/**L5′** (0.240 g, 0.5 mmol) and $CrCl_3(THF)_3$ (0.169 g, 0.45 mmol), **Cr5** was isolated as a brown powder (0.263 g, 92%). FT-IR (cm^{-1}): 2964 (vs), 2930 (s), 2875 (s), 1694 (m), 1612 (m, $\nu_{C=N}$), 1569 (s), 1513 (s), 1457 (vs), 1371 (s), 1324 (m), 1270 (m), 1253 (m), 1202 (m), 1145 (w), 1058 (w), 933 (w), 859 (vs), 830 (m), 797 (m), 761 (s). Anal. Calcd for $C_{33}H_{41}N_3Cl_3Cr$ (638): C, 62.12; H, 6.48; N, 6.59. Found: C, 62.07; H, 6.56; N, 6.39.

Ethylene Polymerization

Evaluation at 1 atmosphere of ethylene pressure Pre-catalyst **Cr2** (2.5 mg, 4.0 μmol) was added to a Schlenk vessel, equipped with a stir bar, followed by freshly distilled toluene (30 mL) and the required amount of co-catalyst then added by syringe. The reaction mixture was stirred at 1 atm. of ethylene pressure at 80 °C. After 30 min., the reaction was quenched with 10% hydrochloric acid in ethanol. The polymer was washed with ethanol, then dried under reduced pressure at 50 °C and weighed.

Evaluation at 5/10 atmospheres of ethylene pressure The higher pressure polymerization runs were carried out in a stainless steel autoclave (0.25 L) equipped with an ethylene pressure control system, a mechanical stirrer and a temperature controller (water or ice-water bath). At the designated reaction temperature, freshly distilled toluene (30 mL) was injected into the autoclave, followed by the complex (4.0 *μ*mol) dissolved in toluene (50 mL). The required amount of co-catalyst was then injected and finally more toluene (20 mL) introduced. The autoclave was immediately pressurized to the designated ethylene pressure and the stirring commenced. After the required reaction time, the ethylene pressure was vented, the reaction was quenched with 10% hydrochloric acid in ethanol. The polymer was washed with ethanol and then dried under reduced pressure at 50 °C and weighed.

X-ray crystallographic studies

Table 5. Crystal data and structure refinement for **Cr2**

Empirical formula	$C_{31}H_{37}Cl_3CrN_3$
Formula weight	609.99
Temperature/ K	173.1500
Wavelength/ Å	0.71075
Crystal system	monoclinic
space group	$P2_1/c$
a/Å	11.608 (2)
b/Å	16.419 (3)
c/Å	16.994 (3)
Alpha/°	90.00
Beta/°	97.48 (3)
Gamma/°	90.00
Volume/Å^3	3211.3 (11)
Z	4
D_{calcd}/ (g cm^{-3})	1.262
μ/mm^{-1}	0.629
F(000)	1276.0
Crystal size /mm	0.192 × 0.185 × 0.119
2θ range /°	3.464 to 50.4
Limiting indices	-13 ≤ h ≤ 13, -19 ≤ k ≤ 19, -20 ≤ l ≤ 20
No. of rflns collected	36218
No. unique rflns [*R*(int)]	5774 [R_{int} = 0.0532, R_{sigma} = 0.0329]
Completeness to θ	100.0%
Data/restraints/parameters	5774/0/348
Goodness of fit on F^2	1.202
Final *R* indices [$I>2\Sigma(I)$]	R_1 = 0.0788, wR_2 = 0.1777
R indices (all data)	R_1 = 0.0817, wR_2 = 0.1795
Largest diff. peak and hole (e Å^{-3})	0.53/-0.41

Crystals of **Cr2** suitable for a single crystal X-ray diffraction determination was obtained by slow diffusion of heptane into a dichloromethane solution of the complex at room temperature. X-ray studies were carried out on a Rigaku Saturn724 + CCD with graphite-monochromatic Mo-Kα radiation (λ = 0.71073 Å) at 173(2) K; cell parameters were obtained by global refinement of the positions of all collected reflections. Intensities were corrected for Lorentz and polarization effects and empirical absorption. The structures were solved by direct methods and refined by full-matrix least squares on F^2. All hydrogen atoms were placed in calculated positions. Structure solution and refinement were performed using the Olex2 1.2 package.[21] Details of the X-ray structure determinations and refinements are provided in Table 5. CCDC 1551376 contains the supplementary crystallographic data for complex **Cr2**. The data can be obtained free of charge from The Cambridge Crystallographic Data Centre via www.ccdc.cam.ac.uk/data_request/cif.

Acknowledgements

This work was supported by the National Natural Science Foundation of China (no. U1362204, 21473160, and 21374123). G. A. S. thanks the Chinese Academy of Sciences for a Visiting Scientist Fellowship.

Keywords: Homogeneous catalysis • Chromium • Polymerization • vinyl group • Thermostability

[1] a) S. D. Ittel, L. K. Johnson, M. Brookhart, *Chem. Rev.* **2000**, *100*, 1169–1203; b) V. C. Gibson, S. K. Spitzmesser, *Chem. Rev.* **2003**, *103*, 283–315; c) S. Mecking, *Angew. Chem. Int. Ed.* **2001**, *40*, 534–540; d) D. S. McGuinness, *Chem. Rev.* **2011**, *111*, 2321; e) T. Agapie, *Coord. Chem. Rev.* **2011**, *255*, 861–880; f) M. P. McDaniel, *Adv. Catal.* **1985**, *33*, 47–98; g) M. P. McDaniel, *Adv. Catal.* **2010**, *53*, 123–606; h) Z. Wang, Q. Liu, G. A. Solan, W.-H. Sun, *Coord. Chem. Rev.* **2017**, *NOI*: 10.1016/j.ccr.2017.06.003.

[2] a) J. T. Dixon, M. J. Green, F. M. Hess, D. H. Morgan, *J. Organomet. Chem.* **2004**, *689*, 3641–3668; b) K. P. Bryliakov, E. P. Talsi, *Coord. Chem. Rev.* **2012**, *256*, 2994–3007; c) V. Katla, S. Du, C. Redshaw, W.-H. Sun, *Review of Catalysts* **2014**, *1 (1)*: 1–14.

[3] Z. Hao, B. Xu, W. Gao, Y. Han, G. Zeng, J. Zhang, G. Li, Y. Mu, *Organometallics* **2015**, *34*, 2783–2790.

[4] a) R. D. Köhn, M. Haufe, G. Kociok-Köhn, S. Grimm, P. Wasserscheid, W. Keim, *Angew. Chem. Int. Ed.* **2000**, *39*, 4337–4339; b) R. D. Köhn, M. Haufe, S. Mihan, D. Lilge, *Chem. Commun.* **2000**, 1927–1928; c) A. K. Tomov, J. J. Chirinos, R. J. Long, V. C. Gibson, M. R. J. Elsegood, *J. Am. Chem. Soc.* **2006**, *128*, 7704–7705; d) Y. Chen, W. Zuo, P. Hao, S. Zhang, K. Gao, W.-H. Sun, *J. Organomet. Chem.* **2008**, *693*, 750–762; e) L. Xiao, M. Zhang, W.-H. Sun, *Polyhedron* **2010**, *29*, 142–147.

[5] a) B. L. Small, M. J. Carney, D. M. Holman, C. E. O'Rourke, J. A. Halfen, *Macromolecules* **2004**, *37*, 4375–4386; b) W. Zhang, W.-H. Sun, X. Tang, T. Gao, S. Zhang, P. Hao, J. Chen, *J. Mol. Catal. A*: *Chem.* **2007**, *265*, 159–166.

[6] J. Liu, Y. Li, J. Liu, Z. Li, *J. Mol. Catal. A*: *Chem.* **2006**, *244*, 99–104.

[7] R. J. Baker, P. G. Edwards, *J. Chem. Soc. Dalton Trans.* **2002**, 2960–2965.

[8] a) A. Carter, S. A. Cohen, N. A. Cooley, A. Murphy, J. Scutt, D. F. Wass, *Chem. Commun.* **2002**, 858–859; b) M. E. Bluhm, O. Walter, M. Döring, *J. Organomet. Chem.* **2005**, *690*, 713–721; c) A. Bollmann, K. Blann, J. T. Dixon, F. M. Hess, E. Killian, H. Maumela, D. S. McGuinness, D. H. Morgan, A. Nveling, S. Otto, M. Overett, A. M. Z. Slawin, P. Wasserscheid, S. Kuhlmann, *J. Am. Chem. Soc.* **2004**, *126*, 14712–14713.

[9] a) D. S. McGuinness, P. Wasserscheid, W. Keim, D. Morgan, J. T. Dixon, A. Bollmann, H. Maumela, F. Hess, U. Englert, *J. Am. Chem. Soc.* **2003**, *125*, 5272–5273; b) M. E. Bluhm, O. Walter, M. Döring, *J. Organomet. Chem.* **2005**, *690*, 713–721.

[10] D. S. McGuinness, V. C. Gibson, D. F. Wass, J. W. Steed, *J. Am. Chem. Soc.* **2003**, *125*, 12716–12717.

[11] a) M. A. Esteruelas, A. M. López, L. Méndez, M. Oliván, E. Oñate, *Organometallics* **2003**, *22*, 395–406; b) Y. Nakayama, K. Sogo, H. Yasuda, T. Shiono, *J. Polym. Sci. Part A*: *Polym. Chem.* **2005**, *43*, 3368–3375; c) N. V. Semikolenova, V. A. Zakharov, L. G. Echevskaja, M. A. Matsko, K. P. Bryliakov, E. P. Talsi, *Catalysis Today* **2009**, *144*, 334–340.

[12] a) V. K. Appukuttan, Y. Liu, B. C. Son, C. Ha, H. Suh, I. Kim, *Organometallics* **2011**, *30*, 2285–2294; b) W. Zhang, W. Chai, W.-H. Sun, X. Hu, C. Redshaw, X. Hao, *Organometallics* **2012**, *31*, 5039–5048; c) W.-H. Sun, S. Kong, W. Chai, T. Shiono, C. Redshaw, X. Hu, C. Guo, X. Hao, *Appl. Catal. A*, *General* **2012**, *67–73*, 447–448; d) J. Ba, S. Du, E. Yue, X. Hu, Z. Flisak, W.-H. Sun, *RSC Adv.* **2015**, *5*, 32720–32729; e) F. Huang, Q. Xing, T. Liang, Z. Flisak, B. Ye, X. Hu, W. Yang, W.-H. Sun, *Dalton Trans*. **2014**, *43*, 16818–16829; f) F. Huang, W. Zhang, E. Yue, T. Liang, X. Hu, W.-H. Sun, *Dalton Trans*. **2016**, *45*, 657–666; g) F. Huang, W. Zhang, Y. Sun, X. Hu, G. A. Solan, W.-H. Sun, *New J. Chem.* **2016**, *40*, 8012–8023; h) Y. Zhang, H. Suo, F. Huang, T. Liang, X. Hu, W.-H. Sun, *J. Polym. Sci. Part A*: *Polym. Chem*. **2017**, *55*, 830–842; i) S. Du, X. Wang, W. Zhang, Z. Flisak, Y. Sun, W.-H. Sun, *Polym. Chem.* **2016**, *7*, 4188–4197; j) S. Du, W. Zhang, E. Yue, F. Huang, T. Liang, W.-H. Sun, *Eur. J. Inorg. Chem*. **2016**, 1748–1755.

[13] C. Huang, S. Du, G. A. Solan, Y. Sun, W.-H. Sun, *Dalton Trans*. **2017**, *46*, 6948–6957.

[14] Y. Zhang, C. Huang, X. Hao, X. Hu, W.-H. Sun, *RSC Adv*. **2016**, *6*, 91401–91408.

[15] a) M. Zhang, K. Wang, W.-H. Sun, *Dalton Trans*. **2009**, 6354–6363; b) S. Zhang, S. Jie, Q. Shi, W.-H. Sun, *J. Mol. Catal. A*: *Chem.* **2007**, *276*, 174–183; c) A. A. Saliu, A. Maliha, M. Zhang, G. Li, W.-H. Sun, *Aust. J. Chem.* **2008**, *61*, 397–403; d) R. Gao, T. Liang, F. Wang, W.-H. Sun, *J. Organomet. Chem*. **2009**, *694*, 3701–3707.

[16] a) B. L. Small, M. Brookhart, A. M. A. Bennett, *J. Am. Chem. Soc*. **1998**, *120*, 4049–4050; b) G. J. P. Britovsek, V. C. Gibson, B. S. Kimberley, P. J. Maddox, S. J. McTavish, G. A. Solan, A. J. P. White, D. J. Williams, *Chem. Commun*. **1998**, 849–850; c) D. J. Jones, V. C. Gibson, S. M. Green, P. J. Maddox, A. J. P. White, D. J. Williams, *J. Am. Chem. Soc*. **2005**, *127*, 11037–11046; d) A. K. Tomov, V. C. Gibson, G. J. P. Britovsek, R. J. Long, M. van Meurs, D. J. Jones, K. P. Tellmann, J. J. Chirinos, *Organometallics* **2009**, *28*, 7033–7040.

[17] a) M. M. Wegner, A. K. Ott, B. Rieger, *Macromolecules* **2010**, *43*, 3624–3633; b) C. Huang, Y. Zhang, T. Liang, Z. Zhao, X. Hu, W.-H. Sun, *New J. Chem.* **2016**, *40*, 9329–9336; c) C. Huang, Y. Zeng, Z. Flisak, Z. Zhao, T. Liang, W.-H. Sun, *J. Polym. Sci. Part A*: *Polym. Chem.* **2017**, *55*, 2071–2083; d) W. Kaminsky, H. Sinn, *Adv. Polym. Sci*. **2013**, *258*, 1–28.

[18] W. Zhang, W.-H. Sun, S. Zhang, J. Hou, K. Wedeking, S. Schultz, R. Fröhlich, H. Song, *Organometallics* **2006**, *25*, 1961–1969.

[19] a) G. B. Galland, R. Quijada, R. Rolas, G. Bazan, Z. J. A. Komon, *Macromolecules* **2002**, *35*, 339–345; b) W.-H. Sun, X. Tang, T. Gao, B. Wu, W. Zhang, H. Ma, *Organometallics* **2004**, *23*, 5037–5047; c) T. Wiedemann, G. Voit, A. Tchernook, P. Roesle, I. Göttker-Schnetmann, S. Mecking, *J. Am. Chem. Soc.* **2014**, *136*, 2078−2085; d) Y. Zhang, H. Li, J.-Y. Dong, Y. Hu, *Polym. Chem*. **2014**, *5*, 105–115; e) N. V. Semikolenova, W.-H. Sun, I. E. Soshnikov, M, A. Matsko, O. V. Kolesova, V. A. Zakharov, K. P. Bryliakov, *ACS Catal.* **2017**, *7*, 2868−2877.

[20] a) W. Herwig, H. Zeiss, *J. Org. Chem.* **1958**, *23 (9)*, 1404; b) J. Jeon, J. Park, D. Park, S. Park, C. Lee, M. Go, J. Lee, B. Lee, *Inorg. Chem. Commun*. **2014**, *44*, 148–150.

[21] O. V. Dolomanov, L. J. Bourhis, R. J. Gildea, J. A. K. Howard, H. Puschmann, *J. Appl. Cryst*. **2009**, *42*, 339–341.

Entry for the Table of Contents (Please choose one layout)

FULL PAPER

The chromium(III) complexes, [2-(ArNCMe)-8-(NAr)C_9H_8N]$CrCl_3$, on activation with MAO or MMAO, show high activitiy towards ethylene polymerization at high temperature and produce highly linear vinyl-polyethylene waxes with narrow distributions (1.1 – 1.8).

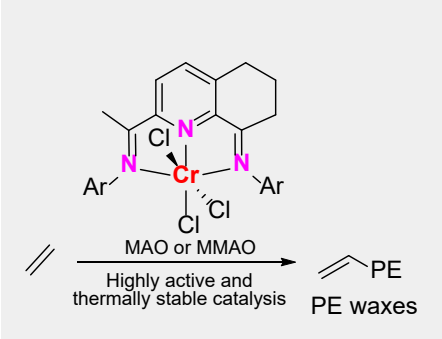

C. Huang, Y. Zhang, G. A. Solan, Y. Ma, X. Hu,* Y. Sun, W.-H. Sun**

Page No. – Page No.

Vinyl-polyethylene waxes with narrow dispersity using a thermally robust bis(imino)trihydroquinolyl-chromium catalyst